SPIRE Spectrometer Bright Mode Gain Calibration Product

Nanyao Lu, Edward Polehampton

1.1 Reference Documents

RD1	SPIRE Bolometer Phase Calibration Product, SPIRE-RAL-NOT-03266, Issue 1, 10 August 2011
RD2	Herschel SPIRE Fourier Transform Spectrometer:Calibration of its Bright-source Mode, Lu et al., Experimental Astronomy, 2014, arXiv:1401.2045

1.2 Introduction

This technical note describes the Spectrometer Bright Mode calibration product, *SCalSpecBrightGain*. The aim of this calibration product is to contain the factors needed to correct observations made using "bright mode" detector settings.

The standard bright mode uses the bolometers with a dephased high bias setting (previously a dephased nominal bias setting was testing during PV phase) – the bright mode settings are described in RD1. Several different schemes have been used for processing bright mode observations, but the final scheme chosen and implemented from HIPE v11 onwards processes bright observations in voltage units using the same RSRF products as for nominal mode. This scheme is described in RD2. Previously, bright mode observations had been processed in temperature units. The following two sections are based on RD2.

1.3 Zero-point Gain Correction

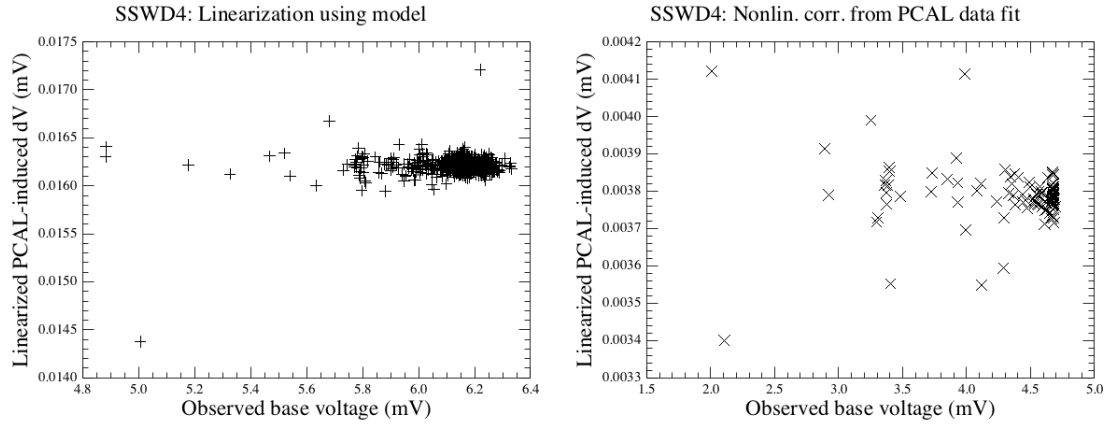

Figure 1: *Linearized PCAL signals for the central detector SSWD4, from the nominal model on the left-hand side and from the bright-source mode on the right.*

Figure 1 shows the linearized PCAL voltages for the detector SSWD4 in the nominal mode (on the left-hand side) and bright-source mode (on the right). These plots also illustrate that, for the majority of the detectors, the typical sample standard deviation for the linearized PCAL signals is of the order of 2% for the bright-source mode and is less than 1% for the nominal mode. Since the linearized voltage is proportional to the optical load on the detector, and the PCAL power and illumination pattern was kept the same for both detector modes, the linearized voltage ratio of the nominal mode to the bright-source mode gives a zero-point gain scaling factor, G_0, from the bright-source to nominal mode. The resulting G_0 varies between 4.1 and 5.4, depending on specific detector.

The mean and median nominal to bright-source were calculated for each detector. Both were very similar and so median ratios were finally used. See Table 1 for the values.

1.4 Frequency-dependent Gain Correction

In addition to G_0, which was derived from low-frequency PCAL signal time lines, we also expect an additional frequency-dependent scaling factor between the two detector setting modes to account for the higher frequency signal modulations in interferograms. This can arise from the fact that bolometer time constant depends on the bias voltage used. While there is a correction for the finite bolometer time constant implemented in the pipeline, any residual effect from imperfect correction could lead to some spectral shape distortion. In the nominal mode, this potential residual spectral shape distortion is simply corrected for at the flux calibration step in the pipeline. To make use of the same flux calibration product for the bright-source mode, we introduced a frequency-dependent gain factor, G_f, which is to be applied to bright-source mode spectra.

Figure 2 shows a number of pair-wise ratios of the nominal to bright-source mode for the two central detectors, SSWD4 and SLWC3, using dark sky spectra taken in the low spectral resolution configuration. Only the zero-point gain correction, G_0, has been applied to the bright-source data here. Each pair of observations were carried out close in time so that the telescope emission, which dominates the signal observed, remained unchanged over the observational pair. The observations used are given in Table 2. Apart from an increased uncertainty at the low frequency end, where the removal of the instrument emission, which is significant only near that end of SLW, introduces additional flux uncertainties, the ratios show approximately a linear dependence on frequency for each detector array. A linear fit was applied to each detector, resulting G_f as a function of frequency.

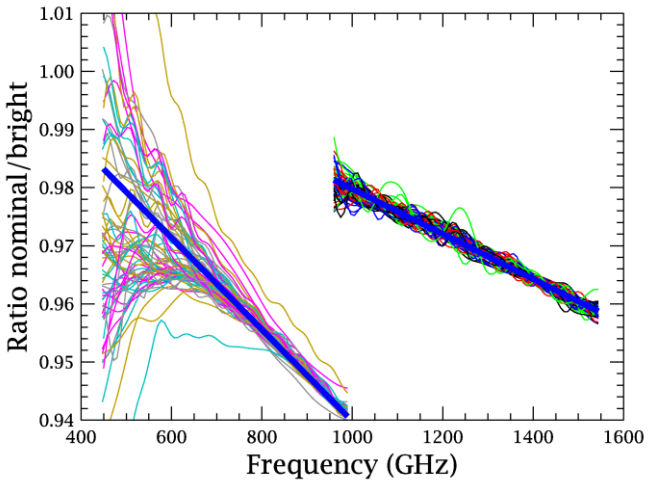

Figure 2: *Frequency dependency of pairwise dark spectrum ratios of the nominal mode to the bright-source mode for the two central detectors, SSWD4 and SLWC3. Only the zero-point gain correction, G_0, was applied to the data of the bright mode here. Independent data pairs are coded in different colors. The spectra have been slightly smoothed in frequency to reduce noise. The two thick blue lines are the best linear fits to the data over SSWD4 and SLWC3, respectively.*

1.5 Calibration product

The calibration product contains columns with the intercept and gradient from the linear fit to the frequency dependent gain, and the nominal to bright PCAL gain, with their errors.

Table 2: *Nominal to Bright PCAL ratios.*

#Detector Median_ratio Mean_ratio Mean_ratio_error Flag
#-------- ------------ ------------ ---------------- ----
Version: 1.1.
Date Stamp: 08 apr 2013.
#
To be used with and ONLY with the following nonlinearity correction products:
(a) nominal nonlinearity product version 4 (dated 07 feb 2011), and
(b) bright nonlinearity product version 5.12 (dated 08 apr 2013).
#

SLWA1	4.50220e+00	4.50407e+00	3.45057e-03	1
SLWA2	4.78986e+00	4.79122e+00	3.87763e-03	1
SLWA3	4.56339e+00	4.55994e+00	6.98106e-03	1
SLWB1	4.54537e+00	4.54452e+00	1.73520e-03	1
SLWB2	4.51749e+00	4.51504e+00	2.56355e-03	1
SLWB3	4.64814e+00	4.64400e+00	3.33622e-03	1
SLWB4	4.42360e+00	4.42282e+00	4.80156e-03	1
SLWC1	4.44028e+00	4.44012e+00	2.22798e-03	1
SLWC2	4.29536e+00	4.29640e+00	1.71451e-03	1
SLWC3	5.13808e+00	5.13868e+00	3.12438e-03	1
SLWC4	4.63545e+00	4.63624e+00	3.29660e-03	1
SLWC5	4.42310e+00	4.42792e+00	6.15057e-03	1
SLWD1	4.55619e+00	4.55458e+00	1.48034e-03	1
SLWD2	4.87443e+00	4.87506e+00	1.63399e-03	1
SLWD3	4.32201e+00	4.31788e+00	2.31025e-03	1
SLWD4	5.05133e+00	5.05413e+00	3.49227e-03	1
SLWE1	4.47314e+00	4.47328e+00	1.64992e-03	1
SLWE2	4.98858e+00	4.98646e+00	1.84608e-03	1
SLWE3	4.50905e+00	4.50881e+00	3.50907e-03	1
SSWA1	4.16205e+00	4.16209e+00	3.44683e-03	1
SSWA2	4.47976e+00	4.47969e+00	3.48184e-03	1
SSWA3	4.23395e+00	4.23931e+00	8.71909e-03	1
SSWA4	4.39932e+00	4.40015e+00	5.26152e-03	1
SSWB1	4.16914e+00	4.17341e+00	2.26391e-03	1
SSWB2	4.31511e+00	4.31721e+00	2.87735e-03	1
SSWB3	4.37877e+00	4.38087e+00	5.00374e-03	1
SSWB4	4.85262e+00	4.85408e+00	1.15779e-02	1
SSWB5	5.00704e+00	5.00211e+00	5.28629e-03	1
SSWC1	4.66490e+00	4.66397e+00	2.36602e-03	1
SSWC2	4.38469e+00	4.38374e+00	2.22107e-03	1
SSWC3	4.20741e+00	4.20836e+00	3.05583e-03	1
SSWC4	4.40178e+00	4.40389e+00	4.09490e-03	1
SSWC5	4.46129e+00	4.45898e+00	4.09758e-03	1
SSWC6	4.25668e+00	4.25954e+00	4.56472e-03	1
SSWD1	4.44179e+00	4.44251e+00	1.63014e-03	1
SSWD2	4.11036e+00	4.10918e+00	2.14416e-03	1
SSWD3	4.63098e+00	4.63286e+00	2.07798e-03	1
SSWD4	4.28517e+00	4.28259e+00	6.04743e-03	1
SSWD5	0.00000e+00	0.00000e+00	0.00000e+00	0
SSWD6	4.26578e+00	4.26576e+00	4.10580e-03	1
SSWD7	4.33242e+00	4.33363e+00	6.78003e-03	1
SSWE1	4.40488e+00	4.40751e+00	1.34674e-03	1
SSWE2	4.36563e+00	4.36507e+00	1.39817e-03	1
SSWE3	4.31772e+00	4.31864e+00	1.84452e-03	1
SSWE4	4.30918e+00	4.30935e+00	2.84400e-03	1
SSWE5	4.81797e+00	4.82165e+00	3.59176e-03	1

SSWE6	4.17776e+00	4.17890e+00	4.88507e-03	1
SSWF1	4.13135e+00	4.13077e+00	1.01309e-03	1
SSWF2	4.97469e+00	4.97487e+00	1.53853e-03	1
SSWF3	5.42523e+00	5.42490e+00	1.98855e-03	1
SSWF4	0.00000e+00	0.00000e+00	0.00000e+00	0
SSWF5	5.22947e+00	5.23208e+00	4.15852e-03	1
SSWG1	5.21029e+00	5.21146e+00	1.72391e-03	1
SSWG2	4.26089e+00	4.26061e+00	1.38057e-03	1
SSWG3	4.35125e+00	4.35222e+00	2.86599e-03	1
SSWG4	4.40340e+00	4.40727e+00	3.64421e-03	1

Table 2: *Observations used to calculate the wavenumber dependent gain.*

Bright Mode	Nominal Mode	Resolution
0x5000400f	0x50004012	HR
0x50005206	0x50005205	HR
0x50005491	0x50005490	HR
0x50005975	0x50005972	HR
0x5000798a	0x50007987	HR
0x50007f43	0x50007f42	HR
0x50008323	0x50008322	HR
0x500088e1	0x500088e0	HR
0x50008d03	0x50008d02	HR
0x500092b1	0x500092b0	HR
0x50009aba	0x50009ab9	HR
0x5000a525	0x5000a524	HR
0x5000ad79	0x5000ad78	HR
0x5000b21a	0x5000b219	HR
0x5000b977	0x5000b976	HR
0x5000c90b	0x5000c90a	HR
0x5000D20D	0x5000D20C	HR
0x5000D5AD	0x5000D5AE	HR
0x5000E948	0x5000E949	HR
0x5000EE24	0x5000EE23	HR
0x5000EFEF	0x5000EFEE	HR
0x5000F275	0x5000F274	HR
0x5000F512	0x5000F511	HR
0x5000FF25	0x5000FF24	HR
0x50010325	0x50010324	HR
0x50010906	0x50010905	HR
0x50010BDE	0x50010BDD	HR
0x50010BE0	0x50010BDD	HR
0x50010D76	0x50010D75	HR
0x50011049	0x50011048	HR
0x500110C6	0x500110C5	HR
0x50011298	0x50011297	HR
0x5001134A	0x50011349	HR
0x5001152C	0x5001152B	HR
0x5001186D	0x5001186C	HR
0x500119EF	0x500119EE	HR
0x50011E18	0x50011E16	HR
0x50012128	0x50012126	HR
0x5001250C	0x5001275D	HR
0x50012B96	0x50012B94	HR
0x500130A7	0x500130A5	HR
0x500133DD	0x500133DB	HR

0x500134EB	0x500134E9	HR
0x500138B9	0x500138B7	HR
0x50013B03	0x50013B01	HR
0x5001417B	0x50014179	HR
0x50014E4C	0x50014E4A	HR
0x500159EF	0x500159EB	HR
0x50010907	0x50010904	LR
0x50010BDF	0x50010BDC	LR
0x50010D77	0x50010D74	LR
0x5001104A	0x50011047	LR
0x500110C7	0x500110C4	LR
0x50011299	0x50011296	LR
0x5001134B	0x50011348	LR
0x5001152D	0x5001152A	LR
0x5001186E	0x5001186B	LR
0x500119F0	0x500119ED	LR
0x50011E17	0x50011E15	LR
0x50012127	0x50012125	LR
0x5001250B	0x50012509	LR
0x50012A57	0x50012A56	LR
0x50012B97	0x50012B95	LR
0x500130A6	0x500130A4	LR
0x500133DC	0x500133D5	LR
0x500134EA	0x500134E8	LR
0x500138B8	0x500138B6	LR
0x50013B02	0x50013B00	LR
0x5001417A	0x50014178	LR
0x50014E4D	0x50014E4B	LR